



**ACCELERATOR EXPERIMENT--Tune versus Beam Position in the Booster**

**Experimentalists:** E. Gray, E.L. Hubbard, F. Mills, R.E. Peters

**Date Performed:** March 15, 1973

Experiment

During late January and the beginning of February 1973, horizontal and vertical tunes were measured versus the horizontal position of the beam by an offset in the rf frequency. At that time only three groups of four sextupoles each were located in the ring (in the long straight sections #3, #11, and #19). The sextupoles were set at a current of +25A during all the acceleration cycle, which cures the beam loss at transition (head-tail effect). Tune data was also taken with the sextupoles off. Large variations of both  $\nu_x$  and  $\nu_y$  were found over a rather small range of  $x$ . The results with the sextupoles off at 1 msec after injection are shown in Fig. 1. The variation of  $\nu_x$  from 6.6 to 6.9 over only 2 cm is spectacular. The failure of attempts to measure tune at larger values of  $x$  suggests two large stopbands at  $\nu = 6.5$  and 7.0 with a width of at least 0.1.

Because (i) the beam width (at least  $\pm 1$  cm) is as large as the aperture in which tune measurements were possible, (ii) the chromaticity varies with azimuth around the ring, (iii) there is a radial closed orbit error as large as 1 cm peak to peak, we thought that the beam decay observed during the first couple of milliseconds might be caused by the large stopbands and the third-order resonance. Previous analysis of the effect of the 30 azimuthal variation of sextupole fields of the lumped sextupole correction magnets yielded only weak resonances, especially on the radial plane.

In early February, another set of 24 air-core sextupoles were installed in the mid-F sections to correct the large radial chromaticity. Tuning of both sets of sextupoles made the decay factor for the first 3 msec change from about 3 to 2. While searching for bad

magnets on February 20, 1973, a rough measurement of the variation of the tune shift was made using the local 3-bump technique at all periods. For the local 3-bump scanning, the three dipole correcting magnets in successive mid-F sections produce a local orbit displacement centered around the period under observation (see Fig. 2). Calculations based on these data showed stopband widths at  $\nu = 6.5$  and  $7.0$  of about  $0.1$  to  $0.2$ , respectively, and a rather large third-order resonance ( $\Delta\nu \sim 0.1$ ). Thus it was recommended that the measurement of the tune versus  $x$  be repeated in a more careful way using the same technique of the local 3 bumps. This experiment was performed:  $\nu_x$  and  $\nu_y$  were measured versus  $x$  at  $0.25$  ms after injection.

During the measurements all sextupoles were at the operating setting (the booster was accelerating beam, and the group of sextupoles in the mid-D sections were powered from about  $15A$  at injection to  $30A$  at transition).

The results of the measurements are shown in Fig. 3. We show in Fig. 4 the horizontal closed orbit (unbumped beam) taken before the tune measurement and in the same condition.

We observe that the closed orbit distortion is at most  $\pm 5$  mm from the pickup center ( $x = 0$ ), the tune variation is now generally small and that the tune measurements took a wider range of  $x$  (in some cases up to  $7$  cm).

### Analysis

We shall limit considerations to the variation of  $\nu_x$  with  $x$ . Let us write the equation of motion on the horizontal plane ( $y = 0$ )

$$x'' + k_0(x)x = G(s,x). \quad (1)$$

An ideal machine should have  $G(s,x) = 0$ . In reality, the presence of this function is motivated by two reasons: (i) There is a contribution from "kinematic" terms which, even for ideal magnets, introduce an intrinsic chromaticity (variation of the tune with the momentum). (ii) To cancel this contribution, a sextupole momentum field is artificially introduced in the magnet profile.

Since in the booster the cancellation is not perfectly done, the function  $G(s,x)$  is the result of this operation.

If we split  $x$  as the sum of the closed orbit  $x_c$  and of the free oscillation  $\xi$ , we have from (1) the following two equations

$$\begin{aligned} x_c'' + k_0(s)x_c &= G(s, x_c) \\ \xi'' + k_0(s)\xi &= G(s, x_c + \xi) - G(s, x_c) \end{aligned} \quad (2)$$

From (2) we can calculate the tune shift  $\Delta v$  in first approximation, assuming small  $\Delta v$  and that we are far away from integer and half-integer tune values:

$$\Delta v = -\frac{1}{4\pi} \int_0^C \beta(s) Q(s, x_c) ds \quad (3)$$

where  $\beta$  is the beatron amplitude function and  $Q(s, x_c)$  is the local gradient error

$$Q(s, x_c) = \lim_{\xi \rightarrow 0} \frac{G(s, x_c + \xi) - G(s, x_c)}{\xi} = \left. \frac{\partial G(s, x)}{\partial x} \right|_{x = x_c}$$

If we take the  $n$ -th period (there are 24 periods in the booster lattice) of 4 magnets as a lumped element, namely, we assume all the 4 magnets have the same closed orbit distortion  $x_n$  (from Fig. 4) and the same (averaged) gradient error  $Q_n(x_n)$ , we have from (3)

$$\Delta v = -\frac{L}{\pi} \bar{\beta} \sum_{n=1}^{24} Q_n(x_n)$$

where  $L$  is the length of a magnet and  $\bar{\beta}$  is the average of  $\beta$  over one period.

In the case now a 3-magnet bump is applied across the  $m$ -th period with a closed orbit distortion of  $x_B$  (averaged over the  $m$ -th period), we have the following tune versus  $x_B$

$$v_m(x_B) = v_0 + \Delta v - \frac{L}{\pi} \bar{\beta} \{Q_m(x_m + x_B) - Q_m(x_m)\}. \quad (4)$$

Since  $v_m$  has been measured versus  $x_B$ , Eq. (4) enables us to estimate the average of the function  $G(s, x_c)$  over the  $m$ -th period, but only above some order.

Let us expand both sides of Eq. (4) in power series around  $x_m$ ,

$$v_m(x_B) = \sum_{\ell=0}^{\infty} b_{m\ell} x_B^{\ell} \quad (5)$$

$$Q_m(x_m + x_B) = \sum_{\ell=0}^{\infty} Q_m^{(\ell)}(x_m) \frac{x_B^{\ell}}{\ell!} \quad (6)$$

where  $Q_m^{(\ell)}(x_m)$  is the average over the  $m$ -th period of

$$\left. \frac{\partial^{\ell+1} G(s, x)}{\partial x^{\ell+1}} \right|_{x = x_c}$$

Inserting (5) and (6) in (4) we have

$$b_{m0} = v_0 + \Delta v$$

$$b_{m\ell} = -\frac{L\bar{\beta}}{\pi \ell!} Q_m^{(\ell)}(x_B), \quad \ell \geq 1 \quad (7)$$

$G(s, x)$ , in power series around  $x_c$ , is

$$G(s, x) = - \sum_{p=0}^{\infty} \frac{B^{(p)}(s, x)}{B\rho} \bigg|_{x=x_c} \frac{(x-x_c)^p}{p!} \quad (8)$$

where  $B\rho$  is the magnetic rigidity and  $B^{(\ell)}$  is the  $\ell$ -pole of the magnetic field around  $x_c$ .

By comparing (7) and (8) we have

$$b_{m\ell} = \frac{L\bar{\beta}}{\pi \ell!} \frac{B_m^{(\ell+1)}}{B\rho} \quad \ell \geq 1$$

Thus the coefficient  $b_{m\ell}$  gives the average  $(\ell+1)$ -pole,  $B_m^{(\ell+1)}$ , in the  $m$ -th period around the average closed orbit  $x_m$ . Also, the data can provide information only about the field momenta higher than the quadrupole.

The coefficients  $b_{m\ell}$  have been calculated with the least square fitting method stopping the series (5) to  $\ell = 4$  and taking into account only the variation of the tune from -15 mm to +15 mm. The results are shown in Table I.

By increasing the whole closed orbit by a factor two or by reducing it by a factor ten, we did not find much variation of the

coefficients  $b_{m\ell}$ . Thus the half-integer stopband widths can be calculated by means of the formula

$$\delta\nu = 2 \left| \sum_{m=1}^{24} \sum_{\ell} b_{m\ell} x_m^{\ell} e^{-iq \frac{\pi}{12} m} \right|.$$

We obtained

$$\delta\nu = 0.002 \text{ for } q = 13 \text{ } (\nu_0 = 6.5)$$

$$\delta\nu = 0.003 \text{ for } q = 14 \text{ } (\nu_0 = 7.0).$$

Observe that these numbers take into account only the combination of high-order moments of the field and closed orbit. Since now they are small, the actual stopbands are likely due to the gradient errors from cell to cell; but these cannot be calculated with the actual tune versus  $x$  data.

We can calculate also the width of higher order resonances, namely,

$$p\nu_0 + q = 0 \quad \text{with} \quad p \geq 3. \quad (9)$$

These resonances divide the phase plane in two regions: in one region (unstable) the motion has an open trajectory, in the other (stable) the motion is periodic. The stable region has a limited area  $S$ . The width of the resonance (9) has the meaning of that range of tune around the resonating value which makes the stable area  $S$  less or, at most, equal to the beam area.

In the approximation the width  $\Delta\nu_{pq}$  of the resonance ( $q$ ) is calculated taking only the contribution from the lowest field moment (for instance, from the sextupole for the third order, from the octupole for  $p = 4$ , and so on), we have, in our case

$$\Delta\nu_{pq} = \frac{\{\sqrt{\epsilon\beta}\}^{p-2}}{2^{p-3}(p-1)} \left| \sum_{n=1}^{24} b_{n,p-2} e^{-iq\phi_n} \right|.$$

Since we have measurement at only 24 locations, at most, we can calculate the width of the third order and (perhaps) of the fourth order resonances.

The results are summarized in the following table

p	q	$\nu_0$	$\Delta\nu_{pq}$
3	20	6.666....	0.004
3	21	7.000....	0.008
4	26	6.500....	0.001
4	27	6.750....	0.001
4	28	7.000....	0.001

### Conclusions

The main result is that after having installed the second set of sextupoles (mid-F sections) and having having powered the first set (mid-D sections), we have now: (a) a small variation of the tune across the vacuum chamber, (b) a wider range of  $x$  across which the tune can be measured, (c) small stopband widths and small third order (likely, also, fourth order) resonance width if we keep the beam in the 3-cm wide corridor around the ring. From this we infer that the beam decay at injection with a single turn injected is not likely caused by the nonlinearities of the field. On the other hand, we should still be concerned about the 4-turn injection because as we can see from Fig. 4 there is a rather large variation of the tune for large  $x$  values. But in this case we cannot extend the present analysis to large  $x$  since, likely, also, the motion on the  $y$ -plane is important.

A suggestion: By using rf bump, measure simultaneously the vertical and radial closed orbit versus  $x$ . This would provide information on the quality of the field versus  $x$  and  $y$ , for large  $x$ , and provide data for calculation of the widths of vertical resonances which may be larger than the widths of the horizontal ones.

A. G. Ruggiero

Table I

n	b <sub>0</sub>	b <sub>1</sub>	b <sub>2</sub>	b <sub>3</sub>	b <sub>4</sub>
1	0.6724E+01	0.9497E-01	0.7817E+01	0.6861E+03	-0.7524E+05
2	0.6725E+01	0.5908E+00	-0.1721E+02	-0.1786E+03	0.2985E+05
3	0.6723E+01	0.2786E+00	-0.2860E+00	0.8328E+03	0.4794E+04
4	0.6724E+01	0.2668E+00	-0.6332E+01	-0.1247E+03	0.1940E+05
5	0.6724E+01	-0.5612E-01	-0.1647E+02	0.1234E+04	0.6818E+05
6	0.6723E+01	0.3027E+00	-0.3243E+01	-0.2709E+03	0.7844E+04
7	0.6723E+01	0.2317E+00	-0.2254E+01	-0.4252E+02	0.2410E+05
8	0.6725E+01	0.2126E+00	-0.2903E+01	-0.2177E+03	0.1681E+05
9	0.6722E+01	0.2270E+00	-0.5500E+00	0.7695E+02	0.1152E+05
10	0.6724E+01	0.5552E+00	0.1508E+01	0.3156E+03	0.2283E+05
11	0.6726E+01	0.3417E+00	0.3095E+01	0.5999E+03	-0.6606E+05
12	0.6724E+01	0.7128E-01	0.1008E+02	0.4153E+02	-0.7765E+05
13	0.6723E+01	0.1607E+00	0.2588E+01	-0.7610E+02	-0.2193E+05
14	0.6724E+01	0.2034E+00	0.4907E+00	-0.1793E+03	-0.1871E+05
15	0.6724E+01	0.1358E+00	-0.9591E+01	-0.7895E+02	0.2633E+05
16	0.6725E+01	0.1270E-02	-0.7768E+00	0.8105E+02	-0.2262E+04
17	0.6725E+01	0.1059E+00	0.5672E+01	0.4968E+02	-0.3463E+05
18	0.6724E+01	0.3680E+00	0.1869E+02	0.6525E+03	-0.1095E+06
19	0.6726E+01	0.3166E+00	-0.6834E+01	0.8074E+03	-0.4724E+04
20	0.6724E+01	0.2041E+00	-0.9233E+01	-0.3170E+03	0.2095E+05
21	0.6723E+01	0.1912E+00	0.2549E+01	-0.7602E+02	-0.2245E+05
22	0.6723E+01	0.1214E+00	-0.6497E+00	0.3737E+03	-0.2628E+05
23	0.6723E+01	0.2157E+00	-0.8579E+00	-0.3129E+02	-0.2156E+05
24	0.6724E+01	0.1357E+00	0.5319E+00	-0.3218E+02	-0.1096E+05

$$B_m^{(l+1)} = 2.1 \cdot l! \cdot b_{ml} \quad (\text{KG/m}^{l+1})$$

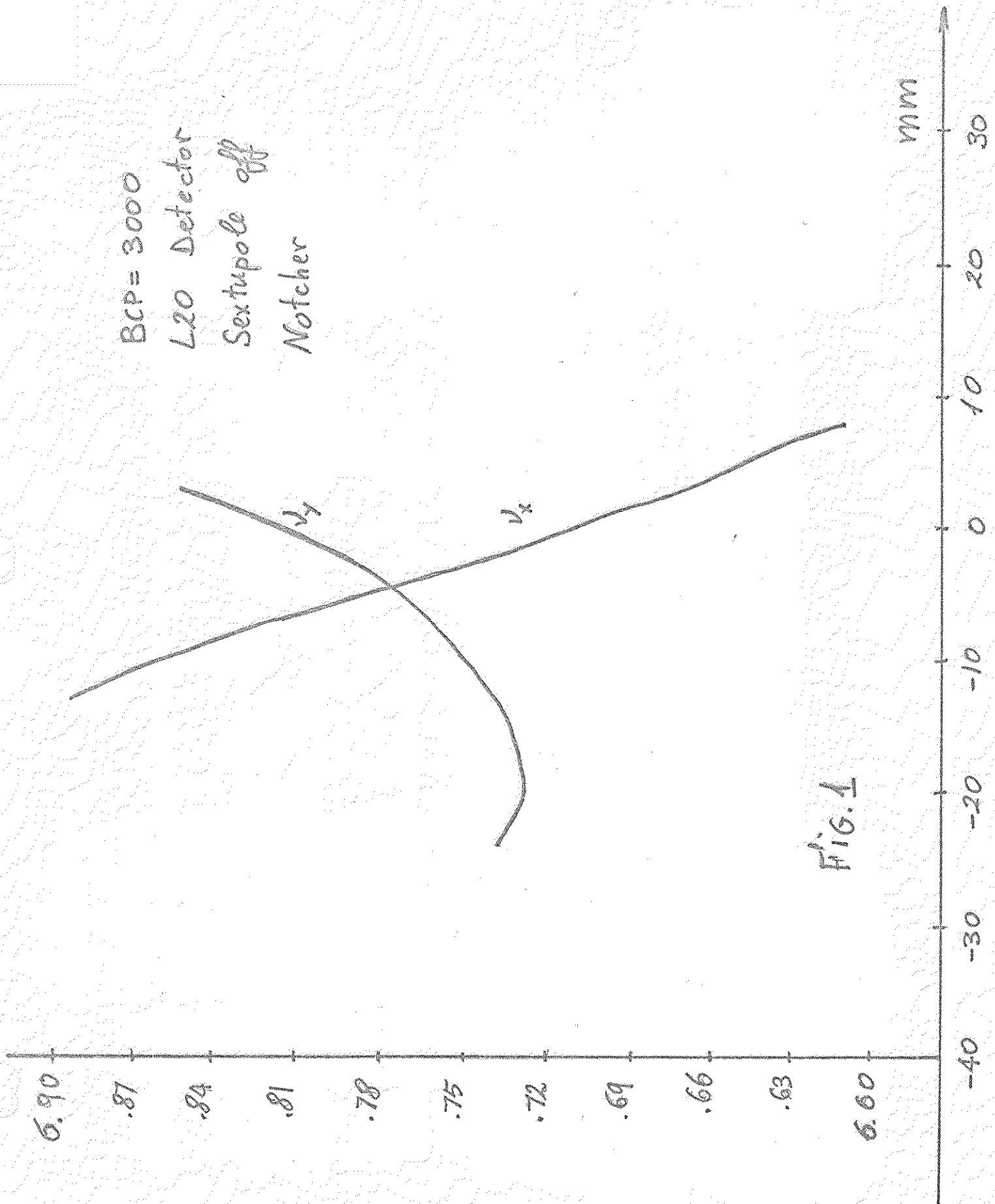
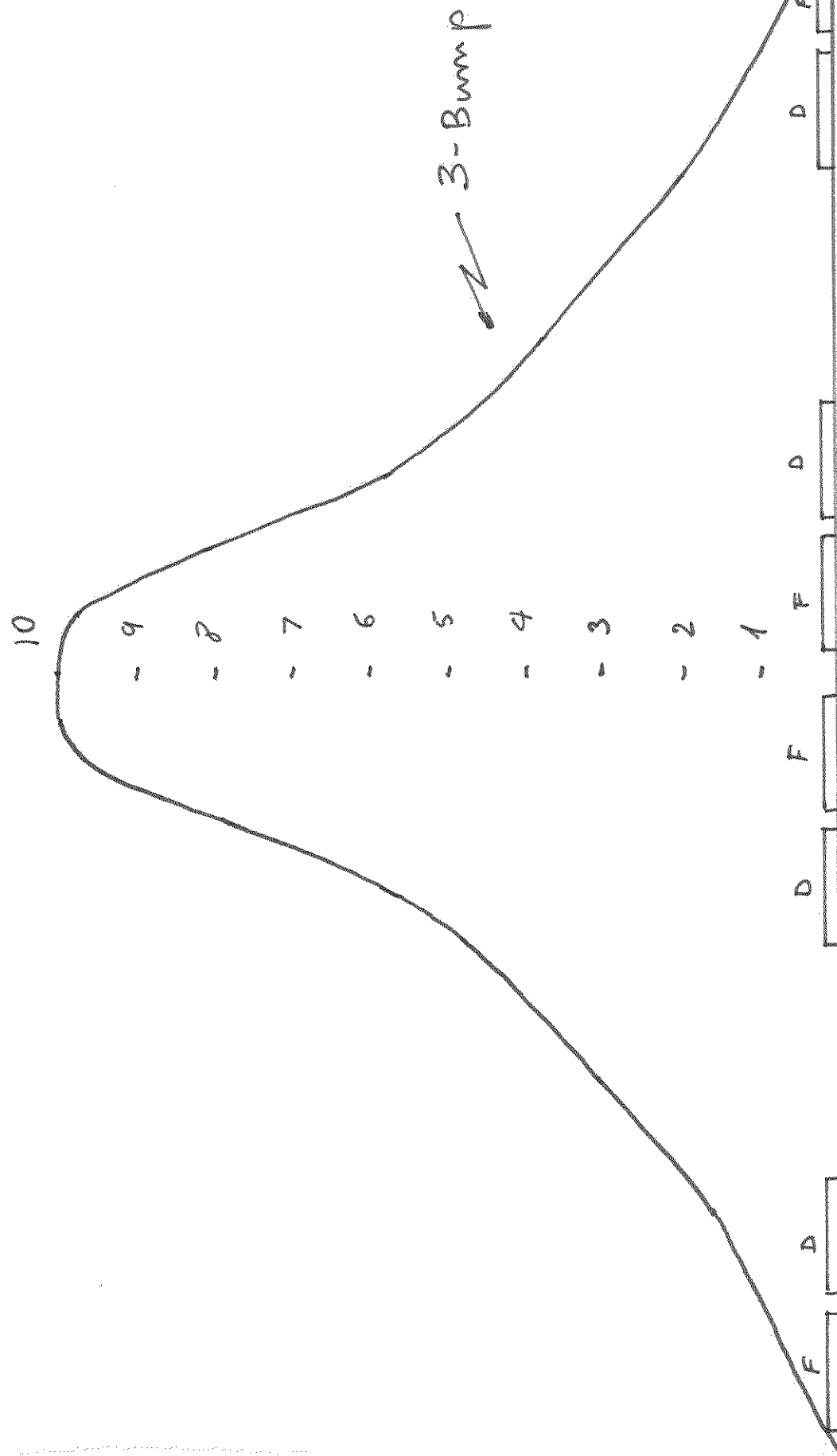




FIG. 2



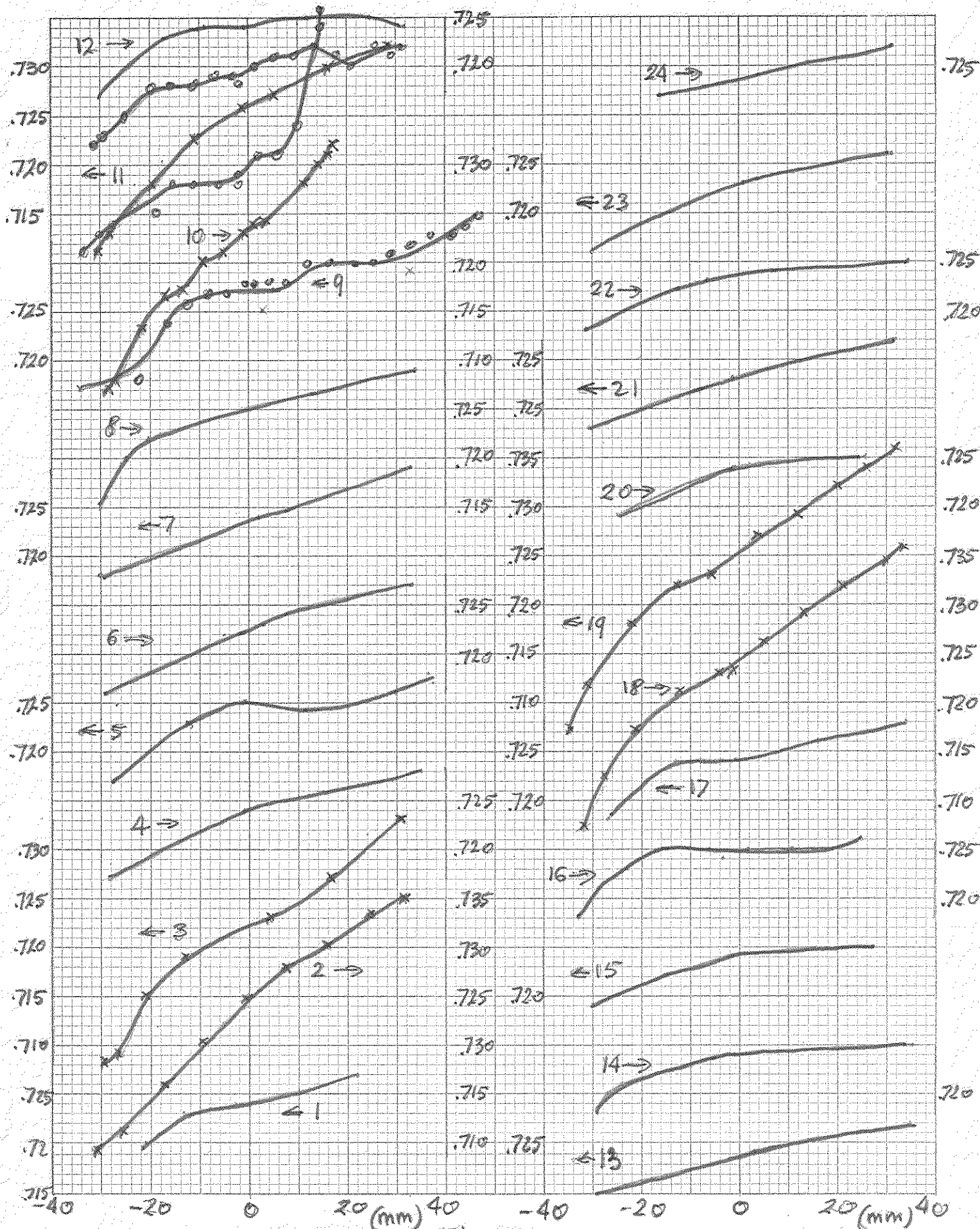


FIG. 3

Clasado bits at 25 Dwell.  
Taken just prior to Bump - time delay

all data points are good

REFUNE INJ CNT=2270		22/15/73 #2:2220		03/15/73 2257	
RADIAL		RADIAL		RADIAL	
L01	-2.805	L09	4.017	L17	1.076
S01	1.143	S09	3.123	S17	1.477
L02	-1.145	L10	4.222	S18	2.635
S02	1.509	S11	3.415	L19	1.165
L03	-4.685	L11	1.872	S19	5.391
S03	1.995	S12	1.432	L20	1.184
L04	-1.044	L12	4.145	S20	1.469
S04	1.022	S13	2.237	L21	3.281
L05	-1.237	L13	3.084	S21	1.331
S05	1.55	S14	1.724	L22	4.427
L06	2.053	L14	1.113	S22	6.168
S06	3.253	S15	2.772	L23	4.071
L07	2.527	L15	1.42	S23	3.58
S07	1.925	S16	3.688	L24	8.55
L08	-1.407			S24	4.321
S08	-1.664				

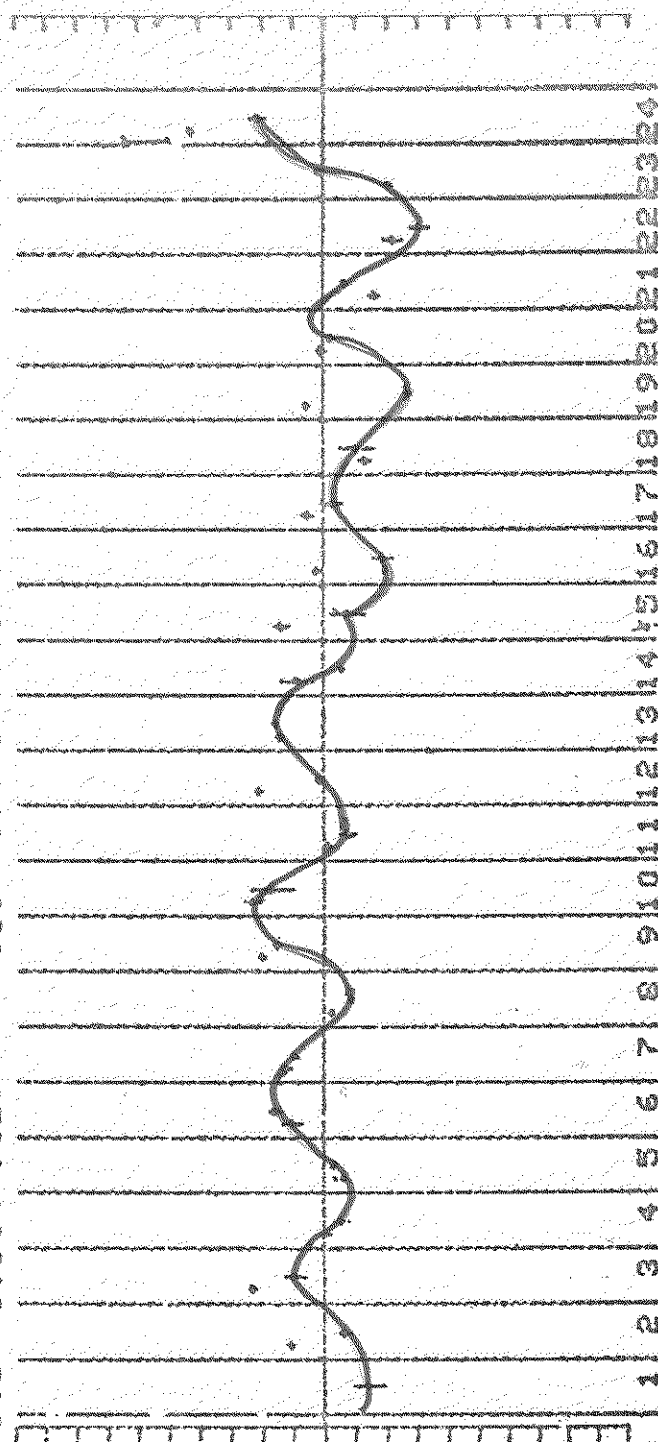


FIG. 4